PUBLIC HEALTH IN THE 21ST CENTURY

THERAPEUTIC ULTRASOUND: MECHANISMS TO APPLICATIONS

VICTOR FRENKEL
EDITOR

Nova Science Publishers, Inc.
New York

In: Therapeutic Ultrasound Mechanisms to Applications ISBN 978-1-61668-599-7
Editor: Victor Frenkel

Chapter 2

THERMAL AND OTHER NON-CAVITATIONAL MECHANISMS

William D. O'Brien, Jr.

ABSTRACT

Ultrasonic biophysics is the study of mechanisms responsible for how ultrasound and biological materials interact. When ultrasound affects biological materials, this can be viewed as a bioeffect, a therapy study and/or a risk. On the other hand, when biological materials affect the ultrasonic wave, this can be viewed as the basis for diagnostic ultrasound. Thus, an understanding of the interaction of ultrasound with tissue provides the scientific basis for understanding the range between risk assessment and image production. Relative to the former, that is, the mechanisms by which it is believed, or known, that ultrasound affects biological materials, ultrasonic bioeffects/therapies are generally separated into thermal and non-thermal mechanisms. The theme of this chapter deals with thermal and other non-cavitational mechanisms of ultrasound, that is, ultrasound-induced effects that are not believed to be bubble related.

1. ULTRASONIC BIOPHYSICS

Ultrasonic biophysics (Dunn and O'Brien, 1976; O'Brien, 2007) is the study of mechanisms responsible for how ultrasound and biological materials interact (Figure 1). The study of how ultrasound affects biological materials can be viewed as bioeffect studies that

can lead to an understanding of therapeutic applications and risk assessments. On the other hand, the study of how tissue affects the ultrasound wave can be viewed as the basis for diagnostic ultrasound. Thus, an understanding of the interaction of ultrasound with tissue provides the scientific basis for understanding image production, therapeutic applications and risk assessment.

Ultrasonic dosimetry (O'Brien, 1978, 1986, 1992b, 1998, 2007) is concerned with the quantitative determination of ultrasonic energy interaction with biological materials, that is, defining the quantitative relationship between some physical agent and the biological effect it produces. To better understand ultrasonic dosimetry and ultrasonic interaction mechanisms, it is appropriate to first introduce basic ultrasonic quantities, and then develop common nomenclature. Then, general dosimetric concepts can be presented because a large body of literature and history exists to quantitate the interaction of various propagated energies and biological materials. This chapter will focus on the noncavitational ultrasound mechanisms, and their corresponding bioeffects, that is, the generation of heat in the context of the therapeutic application of ultrasound and other mechanisms that are not believed to be microbubble or cavitation related. The following chapter (*Acoustic Cavitation*, Chapter 3) will deal exclusively with cavitation and the various phenomena associated with it.

2. BACKGROUND

More than three decades after the 1880 discovery of the piezoelectric effect by the brothers Paul-Jacques and Pierre Curie (Curie and Curie, 1880), a discovery that revolutionized the production and reception of high-frequency sound, the French scientist Paul Langevin developed one of the first uses of ultrasound for underwater echo ranging of submerged objects with a quartz crystal at an approximate frequency of 150 kHz (Hunt, 1982). Langevin was, perhaps, the first to observe that ultrasonic energy could have a detrimental effect upon biological material wherein he reported (Langevin, 1917) "fish placed in the beam in the neighborhood of the source operation in a small tank were killed immediately, and certain observers experienced a painful sensation on plunging the hand in this region."

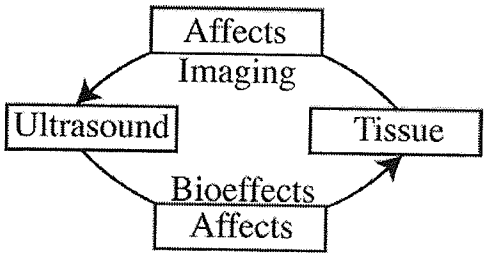

Figure 1. Conceptual diagram of ultrasonic biophysics.

Langevin also reported observing incipient cavitation in water when the source was active, however, he was not the first to propose echo ranging. Incidently, Pierre Curie was Langevin's doctoral thesis advisor. Richardson, in 1912 in response to the Titanic disaster, suggested both airborn (Richardson, 1912a) and underwater (Richardson, 1912b) echo-

ranging schemes, and, in 1914, Fessenden (1914) experimentally demonstrated echo-ranging underwater detection of an iceberg.

Another decade passed before a more detailed, experimental study was conducted (Wood and Loomis, 1927) to investigate Langevin's 1917 observation [A fascinating early history of ultrasound and Alfred Lee Loomis can be found in Jeannet Conant's book *Tuxedo Park: A Wall Street Tycoon and the Secret Palace of Science That Changed the Course of World War II* (Simon and Schuster, 2002)]. Although the ultrasonic levels were not specified, their experimental studies showed that ultrasonic energy had a range of effects from rupture of Spirogyra and Paramecium to death of small fishes and frogs by a one- to two-minute exposure; the latter also observed by Langevin with a Poulsen arc oscillator. Considerable work followed and in the earliest review paper on this subject, Harvey (1930) reported on the physical, chemical, and biological effects of ultrasound in which alterations were produced in macromolecules, microorganisms, cells, isolated cells, bacteria, tissues, and organs with a view towards the identification of the interaction mechanisms. The ultrasonic exposure conditions of these early works were neither well characterized nor reported, but the exposure levels were undoubtedly high.

It is not known when scientists initially recognized the two principal biophysical mechanisms that are currently invoked, viz., thermal and cavitation. The application of ultrasound to therapeutically heat tissue was suggested in the early 1930s (Freundlich et al., 1932) and reported to be used as a physical therapy agent in 1939 (Pohlman et al., 1939). Ultrasound-induced tissue heating was applied extensively as a therapeutic agent in the 1930s and 1940s. However, while it was clear that ultrasound could effectively heat tissue, and excess enthusiasm resulted in numerous clinical applications being proposed and tried, the inferior clinical experience caused this modality to fall into disfavor (see discussion of 1949 Erlangen resolution (Kremkau, 1979)).

Also, during the 1930s and 1940s, with an understanding that ultrasound at sufficient levels could have a dramatic effect on tissues, and produce large temperature increases, the potential for ultrasonic surgery was proposed. This ability to noninvasively burn focal tissue volumes deep in the body using ultrasound was first proposed in 1942 (Lynn et al., 1942, 1944) as a neurosurgery technique. Ultrasound surgery and its biophysical mechanism (heating) were further developed in the late 1940s and early 1950s (Fry et al., 1955). Also proposed in 1948 and applied in 1952 was the application of ultrasound surgery to destroy the vestibular function to treat the symptoms of Menière's disease (Sjoberg et al., 1963).

While ultrasonic exposimetry was inferior in these early times to that possible today, the early bioeffect studies clearly demonstrated that ultrasound, at sufficient levels, could easily destroy biological material. From the earliest considerations that ultrasound might be a feasible energy source for producing images of the human body, it was known that high ultrasonic energy levels had the potential to be therapeutic and/or hazardous.

There have been early ultrasonic dosimetric quantities that are noteworthy of comment in that they represent, in concept, the basic approach to dosimetry. It should be noted that even today there is no adequate dosimetric quantity of therapeutic ultrasound. The *cataract-producing unit*, CPU, was a quantity defined as the length of exposure necessary to produce a grossly observable cataract and expressed in units of seconds (Purnell et al., 1964). The dosimetric concept *damage ability index* with the unit second is a quantity intended to describe the effect of ultrasound on spinal cord hemorrhage (Taylor and Pond, 1972). It has been suggested (Johnston and Dunn, 1976) that a universal dosimetric response to ultrasonic

exposure may exist for different tissues but the response has only been demonstrated, in a limited manner, in mammalian brain tissue. The response was in terms of *energy absorbed per unit volume* for histologically observable lesions at superthreshold levels as a function of the *delivered intensity*. It was shown that at two different ultrasonic frequencies, 3 and 4 MHz, identical constant volume curves resulted even though there were two different threshold levels (Dunn and Fry, 1971). Later, a damage integral was defined to predict the occurrence and dimensions of thermally induced ophthalmic lesions (Lizzi et al., 1984).

During the 1950s and 1960s, the ability to quantify ultrasonic fields improved but only to a limited extent; there were still no national-based ultrasound measurement standards or procedures. All of the improvements dealt with absolute procedures to quantify second-order quantities, and consisted of ultrasonic intensity via thermocouple probe (Fry and Fry, 1954a, 1954b; Fry and Dunn, 1957; Dunn and Breyer, 1962) and electrodynamic method (Filipczynski, 1967), and ultrasonic power via radiation pressure and calorimetry (Wells et al., 1963) and radiation pressure balance (Newell, 1963; Kossoff, 1965).

This period saw only a few advances in our understanding of how ultrasound interacted with biological materials. Perhaps the first major symposium on "Ultrasound in Biology and Medicine" was held at the University of Illinois in 1952 to examine phenomena of how ultrasonic energy interacted with and acted upon biological materials. Of the eight papers presented, six were published and dealt with the effects of high-intensity ultrasound (Fry, 1953; Wall et al., 1953; Wild and Reid, 1953) or the thermal mechanism of ultrasound (Fry and Fry, 1953; Herrick, 1953; Lehmann, 1953). Two additional symposia were held (June, 1955; June, 1962) to address similar issues (Kelly, 1957, 1965). This literature laid the basic foundation for the biophysical mechanisms by which ultrasound is known to affect biological materials, viz., thermal and cavitation.

The 15-year period between early 1970s and mid 1980s witnessed the greatest improvement to quantify ultrasonic fields. These improvements were driven, in part, by the passage in the United States of the 1976 Medical Device Amendments to the Food, Drug and Cosmetic Act. Perhaps the first intercomparison (between two universities) to assess the absolute measurement of ultrasonic intensity was conducted (Breazeale and Dunn, 1974); the comparison was conducted with the elastic sphere radiometer (Dunn et al., 1977). A major breakthrough of earlier work (Brain, 1924; Fukada, 1968) occurred with Kawai's discovery in 1969 (Kawai, 1969) of the strong piezoelectric effect in polyvinylidenefluoride (PVDF) to measure the temporal characteristics of diagnostic ultrasound fields. Two types of PVDF hydrophones were developed, viz., needle (Lewin, 1981) and membrane (DeReggi et al., 1981; Bacon, 1982; Harris, 1982; Preston et al., 1983). The US National Bureau of Standards (now the National Institute of Standards and Technology, NIST) developed an ultrasound power transfer standard (Fick et al., 1984), and the UK National Physical Laboratory developed both a two-transducer reciprocity technique and an optical technique (Smith, 1986).

There have been long-standing national and international standards for therapeutic (physical therapy) ultrasound (Harris, 1992) dating back more than 50 years. Likewise, there have been national and international standards for diagnostic ultrasound that date back to the mid-1980s (Harris, 1992). No national or international standards have been adopted for other therapeutic devices at this time.

3. Basic Ultrasonic Exposure Quantities

Sound is the rapid motion of molecules. These molecular vibrations transport energy from a transmitter, a sound source like our voice, to a receiver like our ear. Sound travels in waves that transport energy from one location to another. When the molecules get closer together, this is called compression, and when they separate, this is called rarefaction. This mechanical motion, the rapid back and forth motion, is the basis for calling sound a mechanical wave or a mechanically propagated wave.

We have many perceptions of the nature of sound. The idea of pitch refers to our perception of frequency, that is, the number of times a second that air vibrates in producing sound that we hear. Voices are classified according to pitch in which the lowest frequency is a bass voice and the highest frequency is a soprano voice. This description of frequency, however, is limited to the frequency range, or spectrum, over which humans can hear sounds. There are sound frequencies below and above what humans can hear. The acoustic spectrum is shown in Figure 2a. The lowest frequency classification in the acoustic spectrum is infrasound that has a frequency range below 20 Hz. Audible sound is what humans hear and has an approximate frequency range between 20 Hz and 20 kHz. The ultrasound frequency range starts at a frequency of 20 kHz. Examples of devices that emit frequencies at the lower frequency end of the ultrasonic spectrum are a dog whistle and industrial ultrasonic cleaners.

Most medical ultrasound equipment operates in the ultrasonic frequency range between 1 and 15 MHz (Figure 2b). Therapeutic (physical therapy, HIFU and ablation) applications operate around 1 MHz. Most imaging applications operate at frequencies greater that about 3 MHz because of the trade-off between spatial resolution and imaging depth.

The classical engineering trade-off of diagnostic ultrasound instrumentation is that between resolution and the depth of the image (or penetration). Both are directly affected by the ultrasonic frequency (f) and attenuation. As frequency is increased, resolution improves and penetration decreases. Resolution improves because the ultrasonic wavelength (λ) in tissue decreases (becomes a smaller number). Wavelength is inversely related to frequency; increase one and the other decreases: $c = \lambda f$ where the tissue's propagation speed, c, is typically assumed to be constant at 1540 m/s.

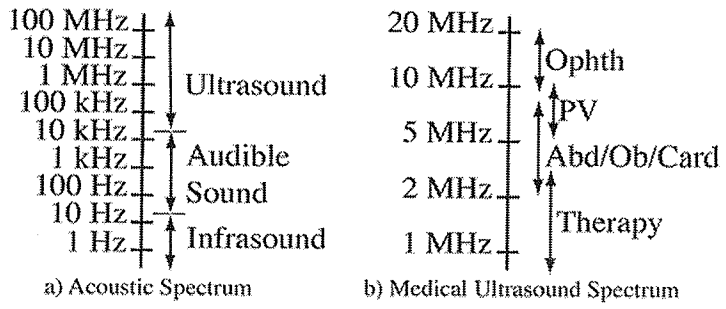

Figure 2. General acoustic spectrum (a) and acoustic spectrum specific for medical ultrasound (b).

As frequency increases, the ultrasonic attenuation also increases. Penetration is directly affected by tissue attenuation because it is approximately linearly related to frequency. At an ultrasonic frequency of 1 MHz, the attenuation coefficient is approximately 0.7 dB/cm

whereas at 2 MHz, it is 1.4 dB/cm. Thus, attenuation coefficient is related to frequency; increase one and the other increases. The attenuation coefficient (also called attenuation slope) can be expressed mathematically by the expression 0.7 dB/cm-MHz, a value that approximately represents soft tissue.

Many of the imaging concepts also apply to therapeutic ultrasound, and thus are introduced here.

A necessary concept to understand axial (or range) resolution is the distance one cycle (and hence one pulse) occupies in a medium. The distance one cycle occupies in a medium is the wavelength. For a pulse waveform, the distance one pulse occupies in a medium is called the spatial pulse length (SPL), that is, the number of wavelengths per pulse ($N\lambda$) where

$$\text{SPL} = N\lambda. \tag{1}$$

Axial resolution is the ability to resolve discrete structures along the beam axis. Quantitatively, it is represented as the minimum distance between two structures at different ranges at which both can just be discretely identified as two separate structures. The best axial resolution is represented by the expression

$$\text{best axial resolution} = \frac{\text{SPL}}{2} = \frac{N\lambda}{2}. \tag{2}$$

The transducer design affects the minimum number of cycles. More highly damped transducers (also referred to as low Q transducers) produce very few cycles of ultrasound when excited by the pulser voltage. As the frequency increases, and other quantities remain constant, axial resolution improves. The term "best axial resolution" has been employed because, in practice, the receiving and processing electronics affect axial resolution as does the quality of the video monitor. The electronics and monitor are often lumped into the term "system Q." Low-valued system Qs provide better axial resolution than do high-valued ones. As a "rule of thumb," there are Q/2 cycles of pressure contained in the pulse, that is, N = Q/2, which yields

$$\text{best axial resolution} = \frac{N\lambda}{2} = \frac{N}{2}\frac{c}{f} = \frac{Q}{4}\frac{c}{f} = \frac{c}{4\Delta f}, \tag{3}$$

where the quality factor Q is defined as the ratio of the center frequency, f, to the system bandwidth, Δf. For a propagation speed of 1540 m/s,

$$\text{best axial resolution (in mm)} = \frac{0.77}{\Delta f}, \tag{4}$$

where Δf is in MHz.

However, ultrasonic images are speckle images and therefore a more representative expression for axial resolution is (Greenleaf and Sehgal, 1992)

$$\text{FWHM}_A \text{ (in mm)} = \frac{1.37}{\Delta f}, \tag{5}$$

where FWHM_A is the axial full width half maximum length of the pulse in millimeters and Δf is in MHz. This expression is also only a function of the system bandwidth but yields a numerical value for axial resolution about 1.8 times greater than the best axial resolution. Thus, the axial resolution improves (its numerical value decreases) when the bandwidth increases.

Lateral resolution is the ability to resolve discrete structures perpendicular, or lateral, to the beam axis. Quantitatively, it is represented as the minimum distance between two side-by-side structures at the same range at which both can just be discretely identified as two separate structures. The best lateral resolution is equal to the minimum beam width; the best lateral resolution term is employed here for the same reasons as that of the term best axial resolution. For a focused ultrasonic field, the beam width (BW) is

$$\text{BW} = 1.4\lambda \frac{\text{ROC}}{\text{D}} = 1.4\lambda f^{\#}, \tag{6}$$

where ROC is radius of curvature (in measurement practice ROC is the distance between the source and the center of the focal region, the focal length) and D is the diameter for a circular source or linear end-to-end lengths for a rectilinear source. In imaging terminology, the term "f-number" or "$f^{\#}$" is often used to quantitate focusing where the lower the f-number value, the better is the focusing. In terms of the full width half maximum length, the beam width at the focus is (Greenleaf and Sehgal, 1992)

$$\text{FWHM}_L \text{ (in mm)} = \frac{\lambda L}{D}, \tag{7}$$

where FWHM_L is the lateral full width half maximum length and L is the focal length (basically the same as ROC.

There are many buzz words to describe a general class of events such as the terms first-order quantity and second-order quantity. Quantity represents what is measured and unit represents the amount (Table 1).

First-order quantities are known as amplitude quantities and second-order quantities as energy-based quantities (Table 2). The basic ideas of first-order and second-order quantities are (1) both first-order and second-order quantities deal with the transport of energy, (2) all first-order quantities are directly proportional to each other, (3) all second-order quantities are directly proportional to each other, and (4) the product of any two first-order quantities is directly proportional to any second-order quantity.

Table 1. Typical ultrasonic quantities and units

Quantity	Unit
charge	coulomb (C)
current	ampere (A = C/s)
displacement	meter (m)
energy	joule (J = Ws)
energy density	joule per meter cubed (J/m3 = N/m2)
force	newton (N)
frequency	hertz (Hz)
intensity	watt per centimeter squared (W/cm2)
length	meter (m)
mass	kilogram (kg)
power	watt (W)
speed	meter per second (m/s)
temperature	degree celsius (°C)
time	second (s)
ultrasonic pressure	pascal (Pa = N/m2)
voltage	volt (V)
wavelength	meter (m)

Table 2. List of first-order and second-order quantities used in ultrasound

First-order quantities	Second-order quantities
current	energy
particle acceleration	energy density
particle displacement	intensity
particle velocity	power
ultrasonic pressure	
voltage	

Acoustic wave propagation, and the development of its wave and other equations (Morse and Ingard, 1968; Nyborg, 1978; Pierce, 1981; Kinsler et al., 1982, 2000; Hall, 1987; Ensminger, 1988; O'Brien, 1992a; Blackstock, 2000), can be approached from the Equation of State which describes the change in density to the change in pressure, the Continuity Equation which relates particle motion to the change in density by invoking conservation of mass and the Momentum Equation (becomes Euler's Equation for a lossless medium at rest) which compares the change in pressure to particle motion through Newton's Second Law of Dynamics by invoking conservation of momentum. These equations and their various forms are:

Equation of State:

$$p = c_o^2 \delta\rho\left\{1 + \frac{B}{2!A}\frac{\delta\rho}{\rho_o} + \frac{C}{3!A}\left(\frac{\delta\rho}{\rho_o}\right)^2 + \mathrm{L}\right\} \tag{8a}$$

$$p = c_o^2 \delta\rho\left\{1 + \frac{B}{2!A}s + \frac{C}{3!A}s^2 + \mathrm{L}\right\} \tag{8b}$$

Continuity Equation:

$$\frac{D\rho}{Dt} + \rho\nabla\cdot\vec{u} = 0 \tag{9a}$$

$$\frac{\partial\rho}{\partial t} + \nabla\cdot(\rho\vec{u}) = 0 \tag{9b}$$

Momentum Equation:

$$\rho\frac{D\vec{u}}{Dt} + \nabla P = 0 \tag{10a}$$

$$\rho_o\frac{\partial\vec{u}}{\partial t} + \nabla p = 0 \text{ (linear Euler's equation)} \tag{10b}$$

The total or material derivative is

$$\frac{Dq}{Dt} = \frac{\partial q}{\partial t} + \vec{u}\cdot\nabla q, \tag{11}$$

where the first term on the right-hand side is the time rate of change of q the fluid particle would experience if it were at rest ($\vec{u} = 0$), and the second term is the additional rate of change caused by the particle's movement. Also, p is the acoustic pressure (instantaneous pressure $P = P_o + p$), $\delta\rho$ is the excess density (instantaneous density $\rho = \rho_o + \delta\rho$), B/A is the coefficient of the first nonlinear parameter (Beyer, 1997), s is the condensation, the fractional change in density ($\delta\rho/\rho_o$) and $\vec{u}$ is the particle velocity of a fluid element.

Pressure P, velocity $\vec{u}$, density ρ can be expressed as

$$P = P_o + p_1 + p_2 + \mathrm{L}\ , \tag{12a}$$

$$\vec{u} = \vec{u}_1 + \vec{u}_2 + \mathrm{L}\ , \tag{12b}$$

$$\rho = \rho_o + \rho_1 + \rho_2 + \mathrm{L}\ , \tag{12c}$$

where the subscripts indicate the order. For example, P_o is the zero-order contribution to pressure, p_1 is the first-order contribution that varies sinusoidally for a harmonic (CW) wave at frequency ω, and p_2 is the second-order contribution that has both a temporal-dependent component at frequency 2ω and a temporal-independent component. Because the fluid is assumed to be at rest, the zero-order contribution to $\vec{u}$ is zero.

The Equation of State, the Continuity Equation and the Euler's Equation for first-order contributions become, respectively,

$$p_1 = Bs_1 + \eta_B \frac{\partial s_1}{\partial t} \tag{13}$$

$$\frac{\partial s_1}{\partial t} = -\nabla \vec{u}_1 \tag{14}$$

$$\rho_o \frac{\partial \vec{u}_1}{\partial t} = -\nabla p_1 \tag{15}$$

In water and tissue, $\eta_B \frac{\partial s_1}{\partial t} << Bs_1$. Thus, the Equation of State becomes $p_1 = Bs_1$. Eliminating the order 1 subscripts and noting that $\vec{u} = \frac{d\vec{\xi}}{dt}$ where $\vec{\xi}$ is the particle displacement, by combining these equations for a one-dimensional wave propagating in the positive x direction yields the one-dimensional lossless wave equation

$$\frac{\partial^2 \xi}{\partial t^2} = c^2 \frac{\partial^2 \xi}{\partial x^2}. \tag{16}$$

The one-dimensional lossless wave equation can be described by the particle displacement $\xi(x,t)$, or can likewise be described by the particle velocity $u(x,t)$, the particle acceleration $a(x,t)$, or the acoustic pressure $p(x,t)$. In terms of the particle displacement, the one-dimensional lossless wave equation traveling in the positive x direction is represented as

$$\xi(x,t) = \xi_o \mathrm{Cos}(\omega t - kx), \tag{17}$$

where ξ_o is the particle displacement amplitude, ω is the angular frequency, t is time and k is the wave number (also called the propagation constant).

For plane waves, particle velocity, particle acceleration and acoustic (ultrasonic) pressure are determined, respectively, from

$$u(x,t)=\frac{\partial\xi(x,t)}{\partial t}, \tag{18}$$

$$a(x,t)=\frac{\partial u(x,t)}{\partial t}, \tag{19}$$

$$p(x,t)=-\rho c^2\frac{\partial\xi(x,t)}{\partial t}, \tag{20}$$

where Eq. 20 is determined by combining the Equation of State and the Continuity Equation to yield $p=\rho_o c^2 s$. All first-order plane wave ultrasonic amplitude quantities are directly proportional to each other. These quantities are

$$\xi_o=\frac{U_o}{\omega}=\frac{A_o}{\omega^2}=\frac{p_o}{\omega\rho_o c_o}, \tag{21}$$

where U_o, A_o and p_o are the particle velocity amplitude, particle acceleration amplitude and acoustic (ultrasonic) pressure amplitude, respectively.

For the lossy wave equation, the medium's attenuation coefficient is part of the solution wherein

$$\xi(x,t)=\xi_o e^{-Ax}\mathrm{Cos}(\omega t-kx), \tag{22}$$

where A is the attenuation coefficient.

When an ultrasound wave propagates in tissue, a mechanical strain is induced, where strain refers to the relative change in dimensions or shape of the body that is subjected to stress. From the second-order contribution to the Momentum Equation, the gradient of P, ∇P, a force quantity, is

$$\vec{F}=\rho\frac{D\vec{u}}{Dt} \tag{23}$$

where $\vec{F}$ is a temporal and spatial varying force per volume (in N/m^3), the volume being a fluid element.

Also, ultrasonic wave propagation transports and dissipates energy, and second-order quantities are proportional to energy. Quantitatively, energy is represented in terms of energy density (a scalar) and intensity (a vector). For a plane wave propagating in the x direction, the instantaneous kinetic and potential energies are, respectively,

$$E_{KE}(x,t)=\frac{\rho u^2}{2}, \tag{24}$$

$$E_{PE}(x,t)=\frac{p^2}{2\rho c^2}, \tag{25}$$

where u and p are the respective instantaneous values of particle velocity and acoustic pressure.

To evaluate the temporal-average energy density, the one-dimensional, harmonically varying particle velocity is assumed to be

$$u(x,t)=U_{op}\mathrm{Cos}(\omega t-kx)+U_{on}\mathrm{Cos}(\omega t+kx), \tag{26}$$

where U_{op} and U_{on} are the particle velocity amplitudes for the positive and negative directed components, respectively, and the one-dimensional, harmonically varying ultrasonic pressure is

$$p(x,t)=p_{op}\mathrm{Cos}(\omega t-kx)+p_{on}\mathrm{Cos}(\omega t+kx), \tag{27}$$

where $p_{op}=\rho cU_{op}$ and $p_{on}=-\rho cU_{on}$. Therefore, the average energy density is

$$\langle E\rangle=\frac{1}{T}\int_0^T E(x,t)dt=\frac{\rho}{2}\left(U_{op}^2+U_{on}^2\right). \tag{28}$$

Intensity is an extremely useful ultrasonic quantity that represents a measure of ultrasonic power flowing (temporal-averaged rate of flow of energy) at normal incidence to a specified unit area. The intensity concept is generally applied in connection with a traveling plane wave. Further, it is a vector quantity but, because the development herein is confined to an isotropic fluid and to the one-dimensional wave equation, vector notation is not used; the direction is known. The instantaneous intensity is defined as the dot product of the ultrasonic pressure and particle velocity but because these two quantities are in phase, the dot product is pu. Its temporal-averaged representation is given by

$$I=\frac{1}{T}\int_0^T pudt=\frac{\rho c}{2}\left(U_{op}^2-U_{on}^2\right). \tag{29}$$

It should be noted that for a standing wave where $U_{op}^2=U_{on}^2$, the temporal-averaged intensity (a vector) is zero whereas the temporal-averaged energy density (a scalar) is not.

For a progressive plane ultrasonic wave propagating in only the positive x direction, $U_{on}^2=0$, and Eqs. 28 and 29 become, letting $U_{op}^2=U_o^2$,

$$\langle E \rangle = \frac{\rho}{2} U_o^2 = \frac{1}{2\rho c^2} p_o^2 \tag{30}$$

and

$$I = \frac{\rho c}{2} U_o^2 = \frac{1}{2\rho c} p_o^2 = \frac{p_o U_o}{2}, \tag{31}$$

where $\langle E \rangle$ is the temporal-average energy density (in J/m^3 or N/m^2) and I is the temporal-avergy intensity (in W/m^2 or, more conventionally in ultrasonic biophysics, W/cm^2). Combining these plane wave results yields

$$\langle E \rangle = \frac{I}{c}, \tag{32}$$

which is an extremely useful expression in terms of measuring ultrasonic intensity and ultrasonic power with radiation force techniques.

The temporal-average energy density is equivalent to the radiation force (in N) for a perfect absorber in that

$$F_{rad} = \frac{IA}{c}, \tag{33}$$

where A is the area of the absorber. The product term IA is acoustic power W, thus,

$$F_{rad} = \frac{W}{c}. \tag{34}$$

For a perfect reflecting surface, the radiation force is twice that of an absorbing target.

If the medium is lossy, and the loss is assumed to be purely absorptive with an absorption coefficient α, then for a one-dimensional wave propagating in the positive x direction, the particle velocity (from Eqs. 18 and 22) and temporal-average intensity can be described by

$$u(x,t) = U_o e^{-\alpha x} \mathrm{Sin}(\omega t - kx), \tag{35}$$

$$I = I_o e^{-2\alpha x}, \tag{36}$$

where I_o is the intensity at x = 0. From these two expressions, and the temporal-average value of $\vec{F}$ (Eq. 23), the temporal-average radiation force on the medium is

$$F_{rad} = \frac{2\alpha I}{c}. \tag{37}$$

4. ULTRASOUND-INDUCED HEATING

Whenever ultrasonic energy is propagated into an attenuating material such as tissue, the amplitude of the wave decreases with distance. This attenuation is due to either absorption or scattering. Absorption is a mechanism that represents that portion of the wave energy that is converted into heat, and scattering can be thought of as that portion which changes direction. Because the medium can absorb energy to produce heat, a temperature increase may occur as long as the rate at which heat is produced is greater than the rate at which the heat is removed (O'Brien, 1978, 2007; NCRP, 1983 1992, 2002). The thermal mechanism is relatively well understood because increase in temperature produced by ultrasound can be calculated using mathematical modeling techniques (Robinson and Lele, 1972; Nyborg, 1975, 1981; Lerner et al., 1973; Cavicchi and O'Brien, 1984, 1985; Nyborg and Steele, 1983; Nyborg and O'Brien, 1989; Curley, 1993) and has been estimated for a variety of exposure conditions (NCRP, 1983, 1992).

In tissue, at the site where the ultrasonic temporal-average intensity is I_{TA}, the average rate of heat generation per unit volume per unit time is given by the expression (Nyborg, 1981; Cavicchi and O'Brien, 1984)

$$Q = 2\alpha I_{TA} = \frac{\alpha p p^*}{\rho c}, \tag{38}$$

where

$$I_{TA} = \frac{p p^*}{2\rho c}, \tag{39}$$

where α is the ultrasonic amplitude absorption coefficient which increases with increasing frequency, p and p* are the instantaneous ultrasonic pressure and its complex conjugate, respectively, ρ is density and c is sound speed. The product of p and p* is equal to the ultrasonic pressure amplitude squared, p_o^2, at the specific location in the medium where Q is determined and can be thought of as a temporal-average quantity.

The temporal-average intensity is not necessarily at the location where it is maximized, that is, at the spatial peak location. If it were, however, then I_{TA} (Eq. 39) would be the spatial peak, temporal peak intensity I_{SPTA}, which would maximize Q for that tissue site. AIUM's Statement on Mammalian In Vivo Ultrasonic Biological Effects (Table 3), sometimes referred to as the *100 mW/cm² Statement*, is a generalization about the state-of-affairs with respect to an intensity-time limit (in terms of I_{SPTA}) below which there have been no independently confirmed significant biological effects in mammalian tissues (AIUM, 2008).

Table 3. American Institute of Ultrasound in Medicine Statement on Mammalian In Vivo Ultrasonic Biological Effects (AIUM, 2008)

Approved November 8, 2008
Information from experiments using laboratory mammals has contributed significantly to our understanding of ultrasonically induced biological effects and the mechanisms that are most likely responsible. The following statement summarizes observations relative to specific diagnostic ultrasound parameters and indices. In the low-megahertz frequency range there have been no independently confirmed adverse biological effects in mammalian tissues exposed in vivo under experimental ultrasound conditions, as follows: 1. Thermal Mechanisms a. No effects have been observed for an unfocused beam having free-field spatial-peak temporal-average (SPTA) intensities* below 100 mW/cm², or a focused** beam having intensities below 1 W/cm², or thermal index values of less than 2. b. For fetal exposures, no effects have been reported for a temperature increase above the normal physiologic temperature, ΔT, when $\Delta T < 4.5 - \log 10\ t\ 0.6$, where t is exposure time ranging from 1 to 250 minutes, including off time for pulsed exposure (Miller et al., 2002). c. For postnatal exposures producing temperature increases of 6°C or less, no effects have been reported when $\Delta T < 6 - \log 10\ t\ 0.6$, including off time for pulsed exposure. For example, for temperature increases of 6.0°C and 2.0°C, the corresponding limits for the exposure durations t are 1 and 250 minutes (O'Brien et al., 2008). d. For postnatal exposures producing temperature increases of 6°C or more, no effects have been reported when $\Delta T < 6 - \log 10\ t\ 0.3$, including off time for pulsed exposure. For example, for a temperature increase of 9.6°C, the corresponding limit for the exposure duration is 5 seconds (=0.083 minutes) (O'Brien et al., 2008). 2. Nonthermal Mechanisms a. In tissues that contain well-defined gas bodies, eg, lung, no effects have been observed for in situ peak rarefactional pressures below approximately 0.4 MPa or mechanical index values less than approximately 0.4. b. In tissues that do not contain well-defined gas bodies, no effects have been reported for peak rarefactional pressures below approximately 4.0 MPa or mechanical index values less than approximately 4.0 (Church et al., 2008).

*Free-field SPTA intensity for continuous wave and pulsed exposures.

**Quarter-power (–6-dB) beam width smaller than 4 wavelengths or 4 mm, whichever is less at the exposure frequency.

For a given I_{TA}, the maximum temperature increase ΔT_{max}, under the assumption that no heat is lost by conduction, convection, or any other heat removal processes, is approximately described by

$$\Delta T_{max} = \frac{Q\,\Delta t}{C_h}, \tag{40}$$

where Δt is the time duration of exposure and C_h is the medium's specific heat. This formula is valid only for short exposure times; for longer exposure times, heat removal processes become significant. Nonetheless, as a "ballpark estimate," using the intensities from the *AIUM Statement* in Table 3 of I_{SPTA} = 0.1 and 1 W/cm^2 at an ultrasonic frequency of 5 MHz, from Eq. 38, Q = 0.05 and 0.5 J/cm^3-s ($\alpha \approx 0.25$/cm at 5 MHz). Because the thermal properties of biological tissue can be approximated by water (C_h = 4.18 J/cm^3-C), the maximum time rates of change of temperature are

$$\frac{\Delta T_{max}}{\Delta t} = 0.012 \text{ and } 0.12\ ^\circ\text{C/s}, \tag{41}$$

which means that for a 1 second exposure, ΔT_{max} would be about 0.012 and 0.12 °C. If the exposure duration were longer than 1 second, the temperature would continue to increase but at a progressively slower rate, until the rate of heat generation was about the same as the rate of heat removal.

To estimate the temperature increase from a single pulse for clinical, diagnostic pulse-echo instrumentation, the local, single pulse intensity of Eq. 38 is considered to be the spatial peak value averaged over the duration of the pulse, that is, the spatial peak, pulse average intensity, I_{SPPA}. For typical instrumentation, a maximum value of I_{SPPA} may be as high as 500 W/cm^2. Thus, the maximum time rate of change of temperature is

$$\frac{\Delta T_{max}}{\Delta t} = 60\ ^\circ\text{C/s}, \tag{42}$$

but, with a diagnostic pulse duration, Δt, of approximately 2 μs, the maximum temperature rise, $\Delta T_{max} \approx 120$ μ°C. However, in the case of high-intensity focused ultrasound (HIFU) for which the spatial peak, pulse average intensity may be 5,000 W/cm^2 the maximum time rate of change of temperature is

$$\frac{\Delta T_{max}}{\Delta t} = 600\ ^\circ\text{C/s}, \tag{43}$$

and for a pulse duration that may be as long as 100 ms, $\Delta T_{max} \approx 60$°C, thus clearly increasing the tissue temperature to a level sufficient for ablation.

There have been several studies to calculate the temperature increase in mammalian tissue from ultrasonic exposure and some of them have shown to compare favorably with experimental results (Pond, 1968, 1970; Robinson and Lele, 1972; Lerner et al, 1973; NCRP, 1983; Nyborg and Steele, 1983; Cavicchi and O'Brien, 1985; AIUM, 1988, 1993, 2000). These demonstrate that selected aspects of the theory are reasonably well understood. But there are still many unanswered concerns in terms of being able to assess in vivo temperature increase, particularly if the goal is to increase the temperature to, say, 43°C, and then hold that 43°C temperature for a period of time.

5. THERMAL DOSE CONCEPT

Healthy cellular activity depends upon chemical reactions occurring at the proper location at the proper rate. The rates of chemical reactions and thus of enzymatic activity are temperature dependent. The overall effect of temperature on enzymatic activity is described by the relationship known as the 10° temperature coefficient, or Q_{10} Rule (Hille, 2001). Many enzymatic reactions have a Q_{10} near 3 which means that for each 10°C increase in temperature, enzymatic activity increases by a factor of 3; a more physical description of rate-dependent temperature effects is the Arrhenius activation energy concept (Henle, 1983; Sapareto and Dewey, 1984; Dewey, 1994; Dewhirst et al., 2003). An immediate consequence of a temperature increase is an increase in biochemical reaction rates. However, when the temperature becomes sufficiently high (i.e., approximately $\geq$ 45°C), enzymes denature. Subsequently, enzymatic activity decreases and ultimately ceases, which can have a significant impact on cell structure and function.

If damage occurs during exposure of tissue(s) to elevated temperature, the extent of damage will be dependent upon the duration of the exposure as well as on the temperature increase achieved. Detrimental or hyperthermia effects in vitro are generally noted at temperatures of 39 to 43°C, if maintained for a sufficient time period; at higher temperatures (> 44°C) coagulation of proteins can occur. These effects have been documented in experimental studies of heat-induced cell death in cultures of normal and cancerous cell lines. The lethal (100% destruction) dose (LD_{100}) for HeLa cells exposed to different temperatures for differing durations has ranged from 41°C for 96-hr duration to 46°C for 30-min duration (Selawry et al., 1957; Hornback, 1984). These findings are comparable to the time-temperature relationship to destroy 50% (LD_{50}) of sarcoma-180 tumor cells in mice (Crile, 1961; Hornback, 1984); from 42°C for 2-hr duration to 46°C for 7.5-min duration.

These observations suggest a logarithmic relationship between time and temperature for death due to a temperature increase. Dickson and Caldwell (1980) have indicated a similar relationship for time vs temperature for thermal-induced death of tumors and normal animal and human tissues. Important points addressed in this study are: (1) at 40°C long-duration exposures (5 to 100 hours) are required for thermal-induced cell death, and (2) at temperatures appreciably below 40°C there were no irreversible adverse effects detected.

An empirical formula, based on a large number of studies involving the thermotolerance of cells and tumors, relates the time, t (in min), required to produce an isoeffect (e.g., a given amount of cell killing) to the time (t_{43}) which would be required had the exposure occurred at a reference temperature of 43°C, that is,

$$t_{43} = t\, R^{(43-T)}, \tag{44}$$

where R = 0.5 for T > 43°C and R = 0.25 for T $\leq$ 43°C (Henle, 1983; Sapareto and Dewey, 1984; Dewey, 1994; Dewhirst et al., 2003). Theoretical considerations based on reaction kinetics (thermodynamic Arrhenius analyses) lead to the prediction that the temperature dependence of the rate of protein denaturation is determined primarily by the activation energy. The quantity R is an expression of the relative increase in reaction rate for a 1°C increase in temperature. The rationale for there being two "R" values is based upon the empirical determinations of R for a number of biological systems and endpoints (Dewey et

al., 1977; Sapareto and Dewey, 1984; Dewey, 1994; Dewhirst et al., 2003). In these systems, R values ranged from 0.4 to 0.8, with 0.5 being the most common value, for temperatures above 43°C. The few studies performed at temperatures ≤ 43°C indicate that the R value is approximately one half of the value obtained at the higher temperatures.

By using Eq. 44, the empirical relationship derived by Sapareto and Dewey (1984), an equivalent t_{43} can be ascribed to any combination of temperature and exposure duration. It also follows that any given biological effect due to hyperthermia can be characterized by that t_{43} value of the causative exposure. The lowest t_{43} value giving rise to some effect would be considered the threshold.

For example, Miller and Ziskin (1989) estimated that the t_{43} was greater than 1 min for each teratologic observation in their study (the lowest t_{43} for any effect was 1.9 min for the production of exencephaly in the mouse (Webster and Edwards, 1984)). Rearranging Eq. 44, and assuming that R = 0.25 (for temperatures ≤ 43°C), yields

$$t = t_{43} 4^{(43-T)}. \tag{45}$$

Miller and Ziskin (1989) used t_{43} = 1 min for fetal tissues, that is,

$$t = 4^{(43-T)}, \tag{46}$$

to indicate that there have been no significant, adverse biological effects observed due to temperature increases less than or equal to the line defined by this equation (see Figure 3); the applicable exposure duration ranged between 1 and 250 min.

For nonfetal tissues a range of t_{43} values has been reported. Results for breast (Lyng et al., 1991) and other tissues (Dewey, 1994) are summarized in Table 4. It should be noted that some of the data were garnered using animal models, whose baseline temperatures are higher than 37°C, implying that the temperature increase necessary to achieve a particular thermal dose would be lower than would be the case with humans (Miller and Dewey, 2003; Herman and Harris, 2003). Adjustments in the t_{43} as applicable to humans might have to be made.

More generally,

$$t = t_{43} R^{(43-T)}, \tag{47}$$

where t is the time (in min) corresponding to the threshold for a specific bioeffect which results from exposure to a temperature T (in °C). Also, R = 0.5 for T > 43°C and R = 0.25 for T ≤ 43°C. This equation explicitly states the relationship between temperature and exposure duration on the boundary line.

Figure 3 shows the temperature-time curves for 4 values of t_{43} (see Eq. 47). The lower curve (t_{43} = 1 min) represents that estimated for fetal tissues for t > 1 min (Miller and Ziskin, 1989; AIUM, 2008; Abramowicz et al., 2008; O'Brien et al., 2008). The other three curves, based on Table 4 t_{43} values (10, 100 and 240 min), represent nonfetal tissues that are less sensitive to tissue damage from temperature. Based on the values in Table 4, the t_{43} = 1 min plot represents a conservative, tissue nonspecific boundary for assessing thermal safety for nonfetal exposures for diagnostic ultrasound applications.

Table 4. t_{43} thermal dose values for various tissues

Tissue	Species	t_{43} (min)
muscle, fat	pig	240
skin	human, rat, mouse	210
esophagus	pig	120
cartilage	rat, mouse	120
breast	human	100
bladder	dog, rabbit	80
small intestine	rat, mouse	40
colon	pig, rabbit	30
liver	dog, rabbit	30
brain	cat, dog	25
kidney	mouse	20

Lyng *et al.*, 1991; Dewey, 1994.

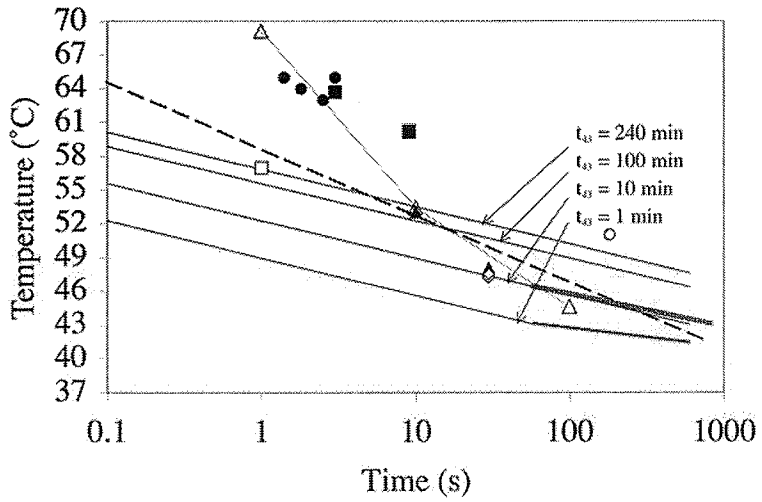

Figure 3. Temperature-time curves (for t_{43}'s of 1, 10, 100 and 240 min) plus the following threshold data (see Table 5): filled-in circle, cat brain; filled-in triangle, rabbit brain; filled-in square, rat brain; open diamond, rabbit muscle; open circle, dog prostate; open square, BHK cells, dashed line, multiple tissue thresholds; shaded line, multiple in vitro thresholds. The red t_{43} = 1 min line denotes a portion of Miller and Ziskin (1989)'s line for t ≥ 60 s.

For very short exposure times, the hyperthermia literature shows only limited (Borelli et al., 1990) t_{43} thermal dose data points for exposure durations of less than 1 min. Two aspects

of single-burst in vivo threshold lesion studies in brain (Fry et al., 1970; Dunn and Fry, 1971; Lerner et al., 1973) and liver (Chan and Frizzell, 1977; Frizzell et al., 1977; Frizzell, 1988) are germane to the thermal dose issue for exposures less than a few seconds. The threshold lesion curve for cat brain is described by the expression $It^{0.5} = 350\ Ws^{0.5}/cm^2$ over for exposure durations between 0.3 ms and 300 sec. The threshold lesion curve for cat and rabbit liver is described by the expression $It^{0.5} = 460\ Ws^{0.5}/cm^2$ over for exposure durations between 3 ms and 35 s. I is the spatial peak intensity (in W/cm^2) and t is exposure duration (in sec). Thus the first aspect is that liver has a higher threshold than brain, consistent with the t_{43} thermal dose trend for brain and liver in Table 4. The second aspect is that for the brain threshold studies, an estimate was made of lesion temperature increase ΔT, yielding, at 6 MHz, $\Delta T/I$ estimates (interpolated from Fig 4 in Lerner et al., 1973) of 0.086, 0.13 and 0.16 $^{\circ}C\text{-}cm^2/W$ for pulse durations of 1, 10 and 100 sec, respectively. Combining these $\Delta T/I$ estimates with $It^{0.5} = 200\ Ws^{0.5}/cm^2$, and assuming a cat core temperature of 39°C (NCRP, 1992), yields three temperature-time data points (filled in circles on Figure 3; also see Table 5).

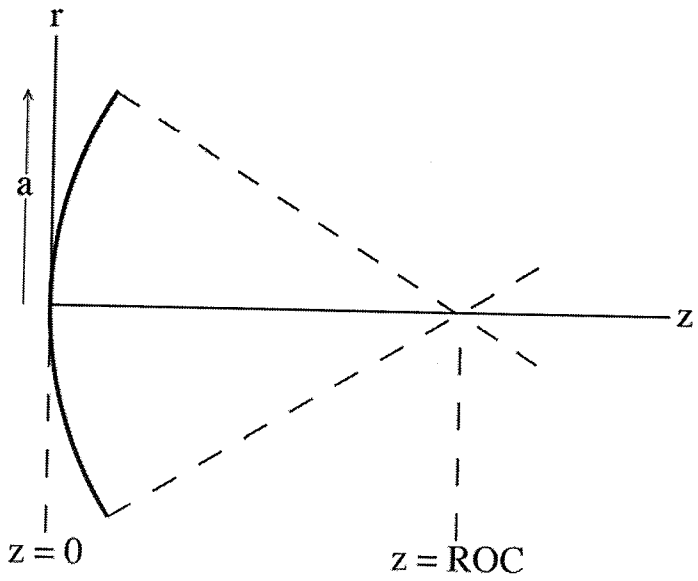

Figure 4. Basic geometry of a spherical disk of radius ROC (radius of curvature) where z = ROC is the geometric focus used to calculate the acoustic field. The radius of the spherical disk in the radial, r, direction is typically denoted by "a", and the f-number is ROC/2a.

In addition, there have been a number of docments that have reported threshold-based data for single-burst exposure durations as low as 100 ms (Table 5). These data are graphically shown in Figure 3.

Table 5. Temperature-time threshold-based data for various biological materials

Figure 3 symbol	Time (s)	Temp (°C)	Material	Reference(s)
Filled-in circle	1	69.1	Cat brain in vivo	Lerner et al., 1973
Filled-in circle	10	53.4	Cat brain in vivo	Lerner et al., 1973
Filled-in circle	100	44.6	Cat brain in vivo	Lerner et al., 1973
Filled-in circle	1.4	65	Cat brain in vivo	Lele, 1977
Filled-in circle	1.8	64	Cat brain in vivo	Lele, 1977
Filled-in circle	2.5	63	Cat brain in vivo	Lele, 1977
Filled-in circle	3	65	Cat brain in vivo	Lele, 1977
Filled-in triangle	10	53	Rabbit brain in vivo	Vykhodtseva et al., 2000
Filled-in triangle	30	48	Rabbit brain in vivo	McDannold et al., 2004
Filled-in triangle	30	47.8	Rabbit brain in vivo	Chen et al., 2002
Filled-in square	9	60.2	Rat brain in vivo	Pond, 1968
Filled-in square	3	63.7	Rat brain in vivo	Pond, 1970
Open diamond	30	47.2	Rabbit muscle in vivo	McDannold et al., 2000
Open diamond	30	47.5	Rabbit muscle in vivo	Cheng et al., 2003
Open circle	180	51	Dog prostate in vivo	Peters et al., 2000
Open square	1	57	BHK cells in vitro	Borelli et al., 1990
Dashed line[1]	0.1	64.5	Multiple tissue thresholds	Lele, 1983
Dashed line[2]	770	41.5	Multiple tissue thresholds	Lele, 1983
Shaded line[1]	60	46.2	Multiple in vitro thresholds	Henle, 1983
Shaded line[2]	840	42.9	Multiple in vitro thresholds	Henle, 1983

[1]Minimum time value is that reported in the article.
[2]Maximum time value was truncated to fit the curve.

These data (Figure 3; Table 5) suggest that for hyperthermia radiation planning, the data base is quite weak and needs considerable attention.

Later on in this book various chapters will deal with specific applications based on the generation of heat. These include reversible effects for healing (*US mediated healing*, Chapter 4) and activating heat senstive promoters for remote control of gene expression (*MR guided HIFU: thermal mapping and gene activation*, Chapter 11), and irreversible effects for hemorrhage control (*Acoustic hemostasis*, Chapter 5) and the destruction of tissue by coagulative necrosis (*US guided HIFU and thermal ablation*, chapter 6). The last chapter (*New research directions and novel applications*, Chapter 13) will also describe how low level hyperthermia generated by HIFU exposures can be used for targeted drug delivery where the heat can deploy drugs from heat sensitive carriers.

6. Non-Cavitational and Non-Thermal Effects

The word "effects" has been used in this section heading because such effects have been identified but the mechanism/mechanisms has/have not been identified.

The ultrasound-induced temporal-average force per volume (Eqs. 23 and 37) has been implicated as a mechanism associated with tactile response (Gavrilov et al. 1977a,b; Gavrilov 1984; Magee and Davies, 1993; Dalecki et al. 1995), auditory response (Foster and Wiederhold 1978; Tsirulnikov et al. 1988), increased fetal activity (Arulkumaran et al., 1991,1996; Saeian et al. 1995; Fatemi et al., 2001), bone repair (Dyson and Brookes, 1983; Wang et al., 1994; Pilla et al., 1990; Wang et al., 2001), tissue regeneration (Dyson et al., 1968, 1970), blood stasis (Dyson et al, 1971, 1974; Nyborg, 1989), cardiac changes in frogs (Dalecki et al., 1993, 1997), movement of detached retinas (Lizzi et al., 1978) and macroscopic streaming to differentiate between cystic and solid tumors (Stavros and Dennis, 1993; Nightingale et al, 1995). Other than those responses related to macrostreaming (Nyborg, 1953, 1965), there is a limited association, possibly only speculation, between the response and radiation force. But, these responses/effects appear to not be caused by bubble activity. In the last chapter (*New research directions and novel applications*, Chapter 13), preliminary evidence will be provided for a proposed novel ultrasound mechanism for enhancing targeted drug delivery - by improving local tissue permeability - where the effects are associated with the creation of radiation forces, and especially the relative large displacements and associated shear that is generated locally in the tissue.

One of the most extensively studied ultrasound-induced biological effects is lung hemorrhage. However, the mechanism is not clear. While heating resulting from the absorption of ultrasound can cause tissue injury, heating has been experimentally excluded as the mechanism responsible for ultrasound-induced lung hemorrhage (Hartman et al., 1992; Zachary et al., 2006). Also, inertial cavitation has been excluded as the mechanism using an overpressure procedure (O'Brien et al., 2000), a pulse polarity procedure (Frizzell et al., 2003) and the injection of contrast agents (Raeman et al., 1997; O'Brien et al., 2004).

7. Delivering Ultrasound

There are three general thermal-based ultrasonic therapy regimes, viz., physical therapy, hyperthermia and ablation. Physical therapy devices generally deliver ultrasound as an unfocused plane wave and ablation devices generally deliver ultrasound as a focused wave. There are no clinically approved hyperthermia devices, given the continuing scientific challenges, and therefore the mode by which ultrasound is delivered is yet to be defined for efficiency.

Textbooks are replete with theory of unfocused plane waves (Beyer and Letcher, 1969; Skudrzyk, 1971; Pierce, 1981; Kinsler et al., 1982, 2000; Hall, 1987; Kino, 1987; Ensminger, 1988; Blackstock, 2000), particularly fields from a plane piston source under harmonic (single frequency) conditions. The resultant and idealized field is divided into two regions, the near or Fresnel region and the far or Fraunhofer region. The distance from the plane piston source that quantifies the length of the near field is commonly taken at the last axial maxima that occurs at a^2/λ where a is the source radius. Other distances have also been

used to designate this distance such as $2a^2/\lambda$ and $\pi a^2/\lambda$ where the axial intensity begins to behave as r^{-2} (r is the distance from the transducer surface); $\pi a^2/\lambda$ is sometimes called the Rayleigh Distance. The ultrasonic fields from physical therapy devices typically deliver ultrasonic energy to tissue under the condition that the tissue is in the near field. For example, if the piston source radius is 1 cm, at a frequency of 1 MHz (λ = 1.5 mm), a^2/λ = 6.7 cm (2.7").

Higher acoustic pressure/intensity values are required for ablative ultrasonic therapy. An example of a spherically focused field (O'Neil, 1949; Stamnes, 1986; Kino, 1987) is useful for demonstrating some basic principles. Figure 4 shows the geometry of the spherically focused transducer with the geometric focus occurring at the depth of focus or the distance of the radius of curvature (ROC). The axial (z direction where r = 0) relative intensity is given by

$$I(r=0,z) \propto \left(\frac{ROC}{z}\right)^2 \mathrm{Sinc}^2\left\{\frac{a^2}{2\lambda ROC}\left(\frac{ROC}{z}-1\right)\right\}, \tag{48}$$

where $\mathrm{Sinc}(X)=\frac{\mathrm{Sin}(\pi X)}{\pi X}$. The lateral (r direction at the focus where z = ROC) relative intensity is given by

$$I(r,z=ROC) \propto \left[\frac{2J_1\left(\frac{kra}{ROC}\right)}{\frac{kra}{ROC}}\right]^2, \tag{49}$$

where J_1 is the Bessel function of the first kind of order 1 and k is the acoustic wave number.

Even when the medium is assumed to be lossless, as in Eqs. 48 and 49, the reciprocal distance parameter in Eq. 48 has a significant influence on where the intensity peaks (Figure 5a). This is why therapy transducers typically are strongly focused (i. e., f/1). Another benefit of a strongly focused field is that the beam width at the focus is relatively narrow (Fig 5b) for a constant frequency. For a lossless medium, frequency does not have a significant influence on where the intensity peaks (Figure 5c), only on the space occupied by the focus (Fig 5c,d).

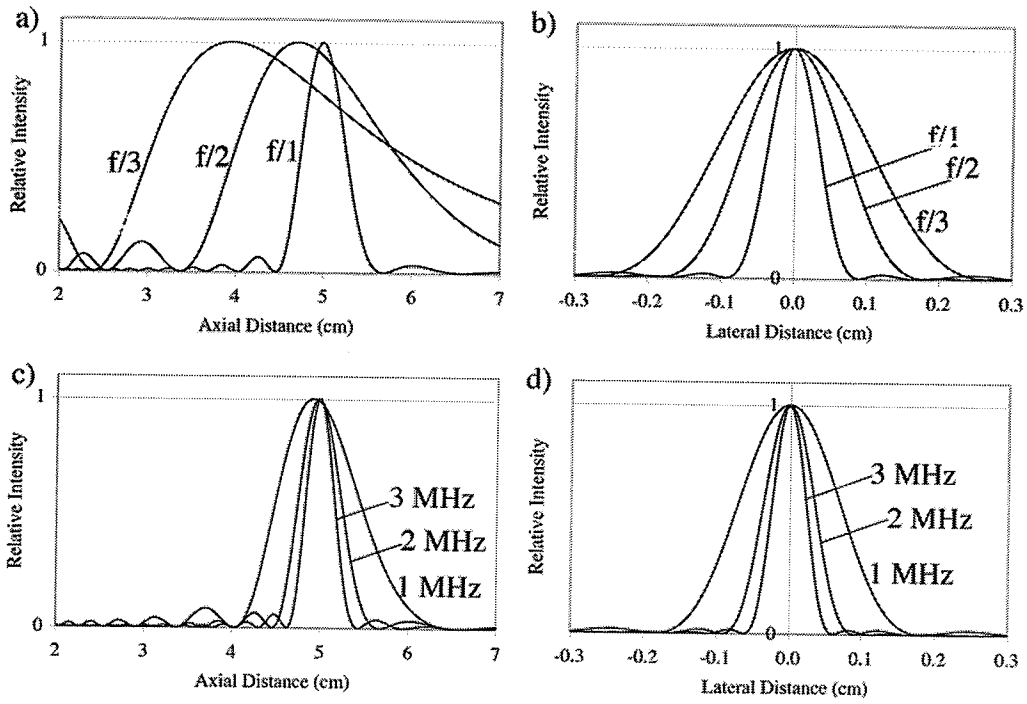

Figure 5. Top panels are the axial (a) and lateral (b) relative intensity plots of the spherically focused field (Eqs. 48 and 49) as a function of f-number (ROC/2a) where frequency is 2 MHz, speed is 1500 m/s and ROC is 5 cm. Botton panels are the axial (c) and lateral (d) relative intensity plots of the spherically focused field (Eqs. 48 and 49) as a function of frequency where the f-number is 2, speed is 1500 m/s and ROC is 5 cm.

ACKNOWLEDGMENTS

This work was supported by NIH R37 EB002641.

REFERENCES

Abramowicz JS, Barnett SB, Duck FA, Edmonds PD, Hynynen KH, Ziskin MC. Fetal thermal effects of diagnostic ultrasound. *J. Ultrasound Med.* 2008;27:541-559.

AIUM, 1987. *AIUM Conclusions Regarding Heat* statement, AIUM Publications, American Institute of Ultrasound in Medicine, 14750 Sweitzer Lane, Suite 100, Laurel, MD 20707, March 26, 1997.

AIUM, 1988. Bioeffects considerations for the safety of diagnostic ultrasound. *J. Ultrasound Med.* 7, September: S1-S38.

AIUM, 1993. Bioeffects and safety of diagnostic ultrasound. American Institute of Ultrasound in Medicine, AIUM Publications, American Institute of Ultrasound in Medicine, 14750 Sweitzer Lane, Suite 100, Laurel, MD 20707.

AIUM, 2000. Mechanical bioeffects from diagnostic ultrasound: AIUM consensus statements. *J. Ultrasound Med.* 19, February: 68-168.

AIUM, 2008. *AIUM Statement on Mammalian In Vivo Ultrasonic Biological Effects*, AIUM Publications, American Institute of Ultrasound in Medicine, 14750 Sweitzer Lane, Suite 100, Laurel, MD 20707, November 8, 2008. Statement available at http://www.aium.org/.

Arulkumaran S, Talbert DG, Nyman M, Westgren M, Hsu TS, Ratman SS. Letter: Audible *in utero* sound from ultrasound scanner. *Lancet* 1991;338:704-705.

Arulkumaran S, Talbert DG, Nyman M, Westgren M, Hsu TS, Ratman SS. Audible *in utero* sound caused by the ultrasonic radiation force from a realtime scanner. *J. Obset Gynaecol. Res.* 1996;22:523–527.

Bacon DR. Characteristics of a PVDF membrane hydrophone for use in the range 1-100 MHz. IEEE Trans Sonics Ultrason 1982;SU-29:18-25.

Beyer RT, Letcher SV. Physical Ultrasonics. New York, NY: Academic Press, 1969.

Beyer RT. Nonlinear Acoustics. Woodbury, NY: Acoustical Society of America, American Institute of Physics, 1997.

Blackstock DT. Fundamentals of Physical Acoustics. New York, NY: Wiley, 2000.

Borrelli MJ, Thompson LL, Cain CA. Dewey WC. Time-temperature analysis of cell killing of BHK cells heated at temperatures in the range of 43.5 °C to 57 °C. *Int. J. Radiation Oncology Biol. Phys.* 1990;19:389-399.

Brain KR. 1924. Investigations of piezo-electric effects with dielectrics. *Proc. Phys. Soc.* (London) 1924;36:81-93.

Breazeale MA. Dunn F. Comparison of methods for absolute calibration of ultrasonic fields. *J. Acoust. Soc. Am.* 1974;55:671-672.

Cavicchi TJ, O'Brien WD Jr. Heat generated by ultrasound in an absorbing medium. *J. Acoust. Soc. Amer.* 1984;70:1244-1245.

Cavicchi TJ, O'Brien WD Jr. Heating distribution color graphics for homogeneous lossy spheres irradiated with plane wave ultrasound. IEEE Trans Sonics Ultrasonics 1985;SU-32:17-25.

Chan SK, Frizzell LA. Ultrasonic thresholds for structural changes in the mammalian liver. Proceedings of the 1977 Ultrasonics Symposium 1977;153-156.

Chen L, Wansapura JP, Heit G, Butts K. Study of laser ablation in the in vivo rabbit brain with MR thermometry. *J. Magn. Reson Imaging* 2002;16:147-152.

Cheng HLM, Purcell VT, Bilbao JM, Plewes DB. Prediction of subtle thermal histopathological change using a novel analysis of Gd-DTPA kinetics. *J. Magn. Reson Imaging* 2003;18,:585-598.

Church CC, Carstensen EL, Nyborg WL, Carson PL, Frizzell LA, Bailey MR. The risk of exposure to diagnostic ultrasound in postnatal subjects: nonthermal mechanisms. *J. Ultrasound Med.* 2008;27:565–592.

Crile G Jr. Heat as an adjunct to the treatment of cancer, experimental studies. Cleveland Clinic Quarterly 1961;28:75-89.

Curie J, Curie, P. Développement par compression de l'électricité polare dans les cristaux hémièdres à faces inclines. Bulletin de la Société Minéralogique de France 1880;3:90-93, and also published in *Comp. Rend.* 1880;91:294-295, 383-386.

Curley MG. Soft Tissue Temperature Rise Caused by Scanned, Diagnostic Ultrasound. IEEE Trans Ultrason Ferroelectr Freq Control 1993;40:59-66.

Dalecki D, Child, SZ, Raeman CH, Carstensen EL. Tactile perception of ultrasound. *J. Acoust. Soc. Am.* 1995;97:3165–3170.

Dalecki D, Keller BB, Raeman CH, Carstensen EL. Effects of ultrasound on the frog heart: I. Thresholds for changes in cardiac rhythm and aortic pressure. *Ultrasound Med. Biol.* 1993;19:385–390.

Dalecki D, Keller BB, Raeman CH, Carstensen EL. Effects of ultrasound on the frog heart: III. The radiation force mechanism. *Ultrasound Med. Biol.* 1997;23:275–285.

DeReggi AS, Roth SC, Kenney JM, Edelman S, Harris GR. Piezoelectric polymer probe for ultrasonic applications. *J. Acoust. Soc. Am.* 1981;69:853-859.

Dewey WC, Hopwood LE, Sapareto SA, Gerweck LE. Cellular responses to combinations of hyperthermia and radiation. *Radiology* 1977;123:463-474.

Dewey WC. Arrhenius relationships from the molecule and cell to the clinic. *Int. J. Hyperthermia* 1994;10:457-483.

Dewhirst MW, Viglianti BL, Lora-Michiels M, Hanson M, Hoppe PF. Basic principles of thermal dosimetry and thermal thresholds for tissue damage from hyperthermia. *Int. J. Hyperthermia* 2003;19:267-294.

Dickson JA, Calderwood SK. Temperature range and selective sensitivity of tumors to hyperthermia: a critical review. In: Jain RK, Gullino PM. eds. Thermal characteristics of tumors: applications in detection treatment. *Ann. of NY Acad. Sci.*: New York 1980;180-205.

Dunn F, Averbuch AJ, O'Brien WD Jr. 1977. A primary method for the determination of ultrasonic intensity with elastic sphere radiometer. *Acustica* 1977;38:58-61.

Dunn F, Breyer JE. Generation and detection of ultra-high-frequency sound in liquids. *J. Acoust. Soc. Am.* 1962;34:775-778.

Dunn F, Fry FJ. Ultrasonic threshold dosages for the mammalian central nervous system. *IEEE Trans Biomed. Engr.* 1971;18:253- 256.

Dunn F, O'Brien WD Jr. Ultrasonic Biophysics, Benchmark Papers in Acoustics. Stroudsberg, PA: Dowden Hutchinson and Ross Inc, 1976.

Dyson M, Brookes M. Stimulation of bone repair by ultrasound. In: Lerski A, Morley P (eds) Ultrasound '82. Elmsford, NY: Pergamon Press, 1983;61–66.

Dyson M, Pond JB, Joseph J, Warwick R. Stimulation of tissue regeneration by means of ultrasound. *Clinical Science* 1968;35:273–285.

Dyson M, Pond JB, Joseph J, Warwick R. Stimulation of tissue regeneration by pulsed, plane wave ultrasound. IEEE Trans Sonics Ultrasonics 1970;SU-17:133-140.

Dyson M, Pond JB, Woodward B, Broadbent J. The production of blood cell stasis and endothelial damage in the blood vessels of chick embryos treated with ultrasound in a stationary wave field. *Ultrasound Med. Biol.* 1974;1:133-148.

Dyson M, Woodward B, Pond JB. Flow of red blood cells stopped by ultrasound. *Nature* 1971;232:572-573.

Ensminger D. Ultrasonics: fundamentals, technology, applications. Second Edition. New York NY: Marcel Dekker Inc, 1988.

Fatemi M, Ogburn PL Jr, Greenleaf JF. Fetal stimulation by pulsed diagnostic ultrasound. *J. Ultrasound Med.* 2001;20:883-889.

Fessenden RA Reported in Hunt (1982) that "this echo-ranging 'first' on April 27, 1914 is recorded in an official report by Captain J. H. Quinan appearing in the U. S. Hydrographic Office Bulletin for May 13, 1914."

Fick SE, Breckenridge FR, Tschiegg CE, Eitzen DG. An ultrasonic absolute power transfer standard. *NBS J. Res.* 1984;8:209-212.

Filipczynski L. The absolute method for intensity measurements of liquid-borne ultrasonic pulses with the electrodynamic transducer. *Proc. Vibr. Probl.* 1967;8:21-26.

Foster KR, Wiederhold ML. Auditory responses in cats produced by pulsed ultrasound. *J. Acoust. Soc. Am.* 1978;63:1199–1205.

Freundlich H, Söllner K, Rogowski F. Einige biologische, wirkungen von ultraschallwellen. (In German. English title: Some biological effects of ultrasound) Klin. Wochenschr. 1932;11:1512-1513.

Frizzell LA, Linke CA, Carstensen EL, Fridd CW. Thresholds for focal ultrasonic lesions in rabbit kidney, liver, and testicle. *IEEE Trans Biomed. Eng.* 1977;24:393-396.

Frizzell LA, Zachary JF, O'Brien WD Jr. Effect of Pulse Polarity and Energy on Ultrasound-induced Lung Hemorrhage in Adult Rats. *J. Acoust. Soc. Am.* 2003;113:2912-2926.

Frizzell LA. Threshold dosages for damage to mammalian liver by high intensity focused ultrasound. IEEE Trans Ultrason Ferroelectr and Freq Control 1988;35:578-581.

Fry FJ, Kossoff G, Eggleton RC, Dunn F. Threshold Ultrasonic Dosages for Structural Changes in Mammalian Brain. *J. Acoust. Soc. Am.* 1970;48:1413-1417.

Fry WJ, Barnard JW, Fry FJ, Krumins RF, Brennan JF. Ultrasonic lesions in the mammalian central nervous system. *Science* 1955;122:517-518.

Fry WJ, Dunn F. Precision calibration of ultrasonic fields by thermoelectric probes. IRE National Convention Record, 1957;Part 9, 39-42. Also published in IRE *Trans Ultrason. Engr.* UE-5, 59-65.

Fry WJ, Fry RB. Determination of absolute sound levels and acoustic absorption coefficients by thermocouple probes – theory. *J. Acoust. Soc. Am.* 1954a;26:296-310.

Fry WJ, Fry RB. Determination of absolute sound levels and acoustic absorption coefficients by thermocouple probes – experiment. *J. Acoust. Soc. Am.* 1954b;26:311-317.

Fry WJ, Fry RB. Temperature changes produced in tissue during ultrasonic irradiation. *J. Acoust. Soc. Am.* 1953;256-11.

Fry WJ. Action of ultrasound on nerve tissue - A review. *J. Acoust. Soc. Am.* 1953;25:1-5.

Fukada E. Piezoelectricity in polymers and biological materials. *Ultrasonics* 1968;6:229-234.

Gavrilov LR, Gershuni GV, Ilyinski OB, Tsirulnikov EM, Shchekanov EE. A study of reception with the use of focused ultrasound: I. Effects on the skin and deep receptor structures in man. *Brain Res.* 1977a;135:265–277.

Gavrilov LR, Gershuni GV, Ilyinski, OB, Tsirulnikov EM, Shchekanov EE. A study of reception with the use of focused ultrasound: II. Effects on the animal receptor structures. *Brain Res.* 1977b;135:279–285.

Gavrilov LR. Use of focused ultrasound for stimulation of nerve structure. *Ultrasonics* 1984;22:132–138.

Greenleaf JF, Sehgal CM. Biologic System Evaluation With Ultrasound. Springer Verlag, New York, NY 1992.

Hall DE. Basic acoustics. New York, NY; Harper and Row, 1987.

Harris GR. Sensitivity considerations for PVDF hydrophones using the spot-poled membrane design. *IEEE Trans Sonics Ultrason* 1982;SU-29:370-377.

Harris GR. Ultrasound Safety Standards. In Greene, M. W. (ed), Non-Ionizing Radiation: Proceedings of the Second International Non-Ionizing Radiation Workshop, Canadian Radiation Protection Association, Vancouver, BC, 1992;209-224.

Hartman CL, Child SZ, Penney DP, Carstensen EL. Ultrasonic heating of lung tissue. *J. Acoust. Soc. Am.* 1992;91:513–516.

Harvey EN. Biological aspects of ultrasonic waves: A general survey. *Biol. Bull.* 1930;59:306-325.

Henle KJ. Arrhenius analysis of thermal responses. In Hyperthermia in Cancer Therapy, Strom FK (ed), Boston, MA: GK Hall Medical Publishers, 1983;47-53.

Herman BA, Harris GR. Response to an extended commentary on 'Models and regulatory considerations for transient temperature rise during diagnostic ultrasound pulses' by Herman and Harris, 2002 by Miller and Dewey, 2003. *Ultrasound in Med. and Biol.* 2003;29:1661-1662.

Herrick JF. Temperatures produced in tissues by ultrasound: experimental study using various techniques. *J. Acoust. Soc. Am.* 1953;25:12-16.

Hille B. Ion channels of excitable membranes. Sunderland, MA:Sinauer Associates, Inc., 2001.

Hornback NB. Hyperthermia and cancer; human clinical trial experience. Vols. I and II, Florida: CRC Press, 1984.

Hunt FV. Electroacoustics: The analysis of transduction, and its historical background. New York: Acoustical Society of America, 1982.

Johnston RL, Dunn F. Ultrasonic absorbed dose, dose rate, and produced lesion volume. *Ultrasonics* 1076;14:153-155.

Kawai H. The piezoelectricity of poly (vinylidene fluoride), *Jpn. J. Appl. Phys.* 1969;8:975-976.

Kelly E. (ed) Ultrasonic energy: biological investigations and medical applications. Urbana, IL: University of Illinois Press, 1965.

Kelly E. (ed) Ultrasound in biology and medicine. Publication No. 3, Washington, DC: American Institute of Biological Sciences, 1957.

Kino GS. Acoustic Waves: Devices, Imaging, and Analog Signal Processing. Englewood Cliffs, NJ: Prentice-Hall Inc, 1987.

Kinsler LE, Frey AR, Coopens AB, Sanders JV. Fundamentals of acoustics. Third Edition, New York, NY:Wiley, 1982.

Kinsler LE, Frey AR, Coopens AB, Sanders JV. Fundamentals of Acoustics. Fourth Edition, New York, NY: Wiley, 2000.

Kossoff G. Balance technique for the measurement of very low ultrasonic power outputs. *J. Acoust. Soc. Am.* 1965;38:880-881.

Kremkau FW. Cancer therapy with ultrasound: A historical review. *J. Clin. Ultrasound* 1979;7:287-300.

Langevin P. French Patent No. 505,703. (filed September 17, 1917; issued August 5, 1920)

Lehmann JF. The biophysical mode of action of biologic and therapeutic ultrasonic reactions. *J. Acoust. Soc. Am.* 1953;25:17-25.

Lele PP. Physical aspects and clinical studies with ultrasonic hyperthermia. In Hyperthermia in Cancer Therapy, Strom FK (ed), Boston, MA: G. K. Hall Medical Publishers, 1983;333-367.

Lele PP. Thresholds and mechanisms of ultrasonic damage to "organized" animal tissues. In Symposium on Biological Effects and Characterizations of Ultrasound Sources, Hazzard DG, Litz ML (eds). US Department of Health, Education, and Welfare HEW Publication (FDA) 1977;78-8048:224-239.

Lerner RM, Carstensen EL, Dunn F. Frequency dependence of thresholds for ultrasonic production of thermal lesions in tissue. *J. Acoust. Soc. Amer.* 1973:54:504-506.

Lewin PA. Miniature piezoelectric polymer ultrasonic hydrophone probes. Ultrasonics 1981;19:213-216.

Lizzi FL, Coleman DJ, Diller J, Ostromogilsky M, Chang S, Greenall P. Ultrasonic hyperthermia for ophthalmic therapy. IEEE Trans on Sonics and Ultrasonics 1984;SU-31:473-481.

Lizzi FL, Coleman DJ, Driller J, Franzen LA, Jakobiec, FA. Experimental, ultrasonically induced lesions in the retina, choroid, and sclera. *Invest Ophthalmol Vis. Sci.* 1978; 17: 350-360.

Lyng H, Monge, OR, Bohler PJ, Rofstad EK. Relationships between thermal dose and heat-induced tissue and vascular damage after thermoradiotherapy of locally advanced breast carcinoma. *Int. J. Hyperthermia* 1991;7:403-415.

Lynn JG, Putman TJ. Histology of cerebral lesions produced by focused ultrasound. *Am. J. Pathol.* 1944;20:637-649.

Lynn JG, Zwemer RL, Chick AJ, Miller AF. A new method for the generation and use of focused ultrasound in experimental biology. *J. Gen. Physiol.* 1942;26:179-193.

Magee TR, Davies AH. Auditory phenomena during transcranial Doppler insonation of the basilar artery. *J. Ultrasound Med.* 1993;12:747-750.

McDannold N, Vykhodtseva N, Jolesz FA, Hynynen K. MRI investigation of the threshold for thermally induced blood-brain barrier disruption and brain tissue damage in the rabbit brain. *Magn. Reson in Medicine* 2004;51:913-923.

McDannold NJ, King RL, Jolesz FA, Hynynen KH. Usefulness of MR imaging-derived thermometry and dosimetry in determining the threshold for tissue damage induced by thermal surgery in rabbits. *Radiology* 2000;216:517-523.

Miller MW, Dewey WC. An extended commentary on "Models and regulatory considerations for transient temperature rise during diagnostic ultrasound pulses" by Herman and Harris (2002), *Ultrasound Med. Biol.* 2003;29:1653-1659.

Miller MW, Nyborg WL, Dewey WC, Edwards MJ, Abramowicz JS, Brayman AA. Hyperthermic teratogenicity, thermal dose and diagnostic ultrasound during pregnancy: implications of new standards on tissue heating. *Int. J. Hyperthermia* 2002; 18:361–384.

Miller MW, Ziskin MC. Biological consequences of hyperthermia. *Ultrasound Med. Biol.* 1989;15:707-722.

Morse PM, Ingard, KU. Theoretical Acoustics, New York, NY: McGraw Hill,1968.

NCRP, 1983. Biological effects of ultrasound: Mechanisms and clinical implications. NCRP Report No. 74. National Council on Radiation Protection and Measurement, Bethesda, MD,1983.

NCRP, 1992. Exposure criteria for medical diagnostic ultrasound: I. Criteria based on thermal mechanisms, Report No. 113. Bethesda, MD: National Council on Radiation Protection and Measurements, 1992.

NCRP, 2002. Exposure Criteria for Medical Diagnostic Ultrasound: II. Criteria Based on all Known Mechanisms, Report No. 140, Bethesda, MD: National Council on Radiation Protection and Measurements, 2002.

Newell JA. A radiation pressure balance for the absolute measurement of ultrasonic power. *Phys. Med. Biol.* 1963;8:215-221.

Nightingale, KR, Kornguth PJ, Walker WF, McDermott BA, Trahey GE. A novel ultrasonic technique for differentiating cysts from solid lesions: Preliminary results in the breast. *Ultrasound Med. Biol.* 1995;21:745-751.

Nyborg WL, O'Brien WD Jr. An alternative simple formula for temperature estimate. *J. Ultrasound Med.* 1989;8:653-654.

Nyborg WL, Steele RB. Temperature elevation in a beam of ultrasound. *Ultrasound Med. Biol.* 1983;9:611-620.

Nyborg WL. Acoustic streaming due to attenuated plane waves. *J. Acoust. Soc. Am.* 1953; 25: 68-75.

Nyborg WL. Acoustic streaming. Physical Acoustics vol. 2B, Mason WP. (ed) New York, NY: Academic Press, 1965:265-331.

Nyborg WL. Heat generation by ultrasound in a relaxing medium. *J. Acoust. Soc. Amer.* 1981;70:310-312.

Nyborg WL. Intermediate biophysical mechanics. Menlo Park, CA:Cummings Publishing Co, 1975.

Nyborg WL. Physical principles of ultrasound. In Ultrasound: Its Applications in Medicine and Biology. Fry FJ. (ed), New York, NY: Elsevier, 1978:1-76.

Nyborg WL. Theoretical criterion for acoustic aggregation. Ultrasound in Medicine and Biology 1989;15:93-99.

O'Brien WD Jr, Deng CX, Harris GR, Herman BA, Merritt CR, Sanghvi N, Zachary JF. The risk of exposure to diagnostic ultrasound in postnatal subjects: thermal effects. *J. Ultrasound Med.* 2008;27:517–535.

O'Brien WD Jr, Frizzell LA, Weigel RM, Zachary JF. Ultrasound-induced lung hemorrhage is not caused by inertial cavitation. *J. Acoust. Soc. Am.* 2000;108:1290-1297.

O'Brien WD Jr, Simpson DG, Frizzell LA, Zachary JF. Effect of contrast agent on the incidence and magnitude of ultrasound-induced lung hemorrhage in rats. *Echocardiography* 2004;21:417-422.

O'Brien WD Jr. Assessing the risks for modern diagnostic ultrasound imaging (Invited). *Jpn. J. Appl. Phys*, 1998;37:2781-2788.

O'Brien WD Jr. Biological effects of ultrasound: Rationale for the measurement of selected ultrasonic output quantities. In Echocardiography, A Review of Cardiovascular Ultrasound 3, New York, NY: Futura Publishing Co, 1986:165-179.

O'Brien WD Jr. Introduction to ultrasound. In Greene M W (ed) Non-Ionizing Radiation: Proceedings of the Second International Non-Ionizing Radiation Workshop, Canadian Radiation Protection Association, Vancouver, BC:1992a:127-150.

O'Brien WD Jr. Ultrasonic dosimetry. In Ultrasound: Its Applications in Medicine and Biology. Fry FJ. (ed) New York, NY: Elsevier, 1978:343-391.

O'Brien WD Jr. Ultrasound – Biophysics Mechanisms. Progress in Biophysics and Molecular Biology 2007;93:212-255.

O'Brien WD Jr. Ultrasound dosimetry and interaction mechanisms. In Greene M W (ed) Non-Ionizing Radiation: Proceedings of the Second International Non-Ionizing Radiation Workshop, Canadian Radiation Protection Association, Vancouver, BC, 1992b:151-172.

O'Neil HT. Theory of focusing radiations. *J. Acoust. Soc. Amer.* 1949;21:516-526.

Peters RD, Chan E, Trachtenberg J, Jothy S, Kapusta L, Kucharczyk W, Henkelman RM. Magnetic resonance thermometry for predicting thermal damage: an application of

interstitial laser coagulation in an in vivo canine prostate model. *Magn. Reson. Med.* 2000;44:873-883.

Pierce AD. 1981. Acoustics: An introduction to its physical principles and applications. McGraw Hill, New York, NY. (A 1989 edition is published by the Acoustical Society of America through the American Institute of Physics, Woodbury, NY)

Pilla AA, Mont MA, Nasser PR, Khan SA, Figueiredo M, Kaufman JJ, Siffert RS. Non-invasive low-intensity pulsed ultrasound accelerates bone healing in the rabbit. *J. Orthop. Trauma* 1990;4:246-253.

Pohlman R, Richter R, Parow E. Uber die ausbreitung und absorption des ultraschall im menschlichen gewebe und seine therapeutische wirkung an ischias und plexusneuralgie. *Dtsch med. Wochenschr* 1939;65:251-254.

Pond JB. A Study of the Biological Action of Focussed Mechanical Waves (Focussed Ultrasound). Ph.D. Thesis, London University, 1968.

Pond JB. The role of heat in the production of ultrasonic focal lesions. *J. Acoust. Soc. Am.* 1970;47:1607-1611.

Preston RC, Bacon DR, Livett AJ, Rajendran K. PVDF membrane hydrophone performance properties and their relevance to the measurement of the acoustic output of medical ultrasonic equipment. *J. Phys. E: Sci. Instr.* 1983;16:786-796.

Purnell EW, Solollu A, Torchia R, Taner H. Focal chorioretinitis produced by ultrasound. *Invest Ophth.* 1964;3:657-664.

Raeman CH, Dalecki D, Child SZ, Meltzer RS, Carstensen EL. Albunex does not increase the sensitivity of the lung to pulsed ultrasound. *Echocardiography* 1997;6:553-557.

Richardson LF. "Apparatus for warning a ship at sea of its nearness to large objects wholly or partly under water," British Patent No. 11,125 (filed May 10 , 1912b; issued March 27, 1913)

Richardson LF. "Apparatus for warning a ship of it approach to large objects in a fog," British Patent No. 9423 (filed April 20 , 1912a; issued March 6, 1913).

Robinson TC, Lele PP. An analysis of lesion development in the brain and in plastics by high intensity focused ultrasound at low megahertz frequencies. *J. Acoust. Soc. Amer.* 1972;51: 1333- 1351.

Saeian K, Weintraub R, Hagen-Ansert S, Sahn C, Shiota T, Kenny A, Sahn DJ. Increased fetal activity and heart rate during and immediately after pulsed Doppler echocardiography. *Echocardiography* 1995;12:71–77.

Sapareto SA, Dewey WC. Thermal dose determination in cancer therapy. *Int. J. Radiat. Oncol. Biol. Phys.* 1984;10:787-800.

Selawry OX, Goldstein MW, McCormick T. Hyperthermia in tissue-cultured cells of malignant origin. *Cancer Res.* 1957;17:785-791.

Sjoberg A, Stable J, Johnson S, Sahl R. Treatment of Meniere's disease by ultrasonic irradiation. *Acta Otolaryngol. Suppl.* 1963;178:171-175.

Skudrzyk E. The Foundations of Acoustics. Springer-Verlag, New York, NY, 1971. (The 1971 edition is published by the Acoustical Society of America through the American Institute of Physics, Woodbury, NY)

Smith RA. 1986. The calibration of hydrophones for use in medical ultrasonic fields - A review. NPL Report Ac 108, Teddington, Middlesex, UK: National Physical Laboratory.

Stamnes JJ. 1986. Waves in Focal Regions. IOP Publishing Limited, Bristol, UK.

Stavros AT, Dennis MA. The ultrasound of breast pathology. In Parker, S.H. and Jobe, W.E. (Eds.): Percutaneous Breast Biopsy. Raven Press, New York, 1993:111-115.

Taylor KJW, Pond JB. A study of the production of hemorrhagic injury and paraplegia in rat spinal cord by pulsed ultrasound of low megahertz frequencies in the context of the safety for clinical usage. *Brit. J. Radiol.* 1972;45:343-353.

Tsirulnikov EM, Vartanyan IA, Gersuni GV, Rosenblyum AS, Pudov VI, Gavrilov LR. Use of amplitude-modulated focused ultrasound for diagnosis of hearing disorders. *Ultrasound Med. Biol.* 1988;14:277–285.

Vykhodtseva N, Sorrentino V, Jolesz FA, Bronson RT, Hynynes K. MRI detection of the thermal effects of focused ultrasound on the brain. *Ultrasound Med. Biol.* 2000;26:871-880.

Wall PD, Tucker D, Fry FJ, Mosberg WH. The use of high intensity ultrasound in experimental neurology. *J. Acoust. Soc. Am.* 1953;25:281-285.

Wang C, Chen H, Chen C, Yang K. Treatment of nonunions of long bone fractures with shock waves. *Clin. Orthop. Related Re.* 2001;387:95-101.

Wang SJ, Lewallen DG, Bolander ME, Chao EYS, Ilstrup DM, Greenleaf JF. Low intensity ultrasound treatment increases strength in a rat femoral fracture model. *J. Orthop. Res.* 1994; 12:40-47.

Webster WS, Edwards MJ. Hyperthermia and the induction of neural tube defects in mice. *Teratology* 1984;29:417-425.

Wells PNT, Bullen MA, Follett DH, Freundlich HF, James JA. The dosimetry of small ultrasonic beams. *Ultrasonics* 1963;1:106-110.

Wild JJ, Reid JM. The effects of biological tissues on 15-mc pulsed ultrasound. *J. Acoust. Soc. Am.* 1953;25:270-280.

Wood RW, Loomis AL. The physical and biological effects of high-frequency sound waves of great intensity. *Philos. Mag.* (VII), 1927;4:417-436.

Zachary JF, Blue JP Jr, Miller RJ, Ricconi BJ, Eden JG, O'Brien WD Jr. Lesions of ultrasound-induced lung hemorrhage are not consistent with thermal injury. *Ultrasound Med. Biol.* 2006; 32: 1763-1770.